Proceedings World Geothermal Congress 2010
Bali, Indonesia, 25-29 April 2010

Investigation of Mobility Changes During Water Injection/fall-Off Tests in Liquid-Dominated Geothermal Reservoirs

Abbas Azarkish

7C Grange Rd, Mt Eden, Auckland, New Zealand

azarkish@yahoo.com

Keywords: water injection, fall-off, mobility changes

ABSTRACT

This paper aims at investigating the mobility changes during the water injection/falloff experiment in a liquid dominated geothermal reservoir using both analytical and numerical models. Firstly, the fundamental of water injection/fall-off test calculations will be discussed. Secondly, a case study will be shown to critically compare and demonstrate the pressure and pressure derivative behaviour of the test. Finally, some conclusions will be made.

1. INTRODUCTION

After the discovery of a geothermal field by successfully drilling of one or more wells, the reservoir engineer has to obtain as much information out of them as possible. This information is needed in order to perform a proper evaluation of the field, before the operator company can proceed with the construction of a power generating plant.
Injection/fall-off testing is a pressure transient test during injection into a well. Injection well testing and the associated analysis are essentially simple, as long as the mobility ratio between the injected fluid and the reservoir fluid is unity. Earlougher [1] pointed out that the unit-mobility ratio is a reasonable approximation for many reservoirs under water injections. The objectives of water injection/fall-off tests are similar to those of production tests, namely the determination of:

- permeability
- skin
- average pressure
- reservoir heterogeneity
- front tracking

Injection well testing involves the application of one or more of the following approaches:

- step-rate injectivity test
- pressure falloff test

2. METHODOLOGY

In an injectivity test, the well is shut in until the pressure is stabilized at initial reservoir pressure p_i. At this time, the injection begins at different constant flow rates (q_{inj}), while recording the bottom-hole pressure p_{wf}. For a unit-mobility ratio system, the injectivity test would be identical to a pressure drawdown test except that the constant rate is negative with a value of $-(q_{inj})$.

Sabet [2] pointed out that, depending on whether the density of the injected fluid is higher or lower than the reservoir fluid, the injected fluid will tend to override or under ride the reservoir fluid and, therefore the net pay "h" which should be used in interpreting injection/fall-off tests would not be the same as the net pay which is used in interpreting drawdown tests.

Figure 1 shows a plan view of the saturation distribution in the vicinity of an injection well in non-unit mobility ratio systems. This figure shows two distinct zones. Zone-1 represents the water bank with its leading edge at a distance of r_1 from the injection well. The mobility λ of the injected fluid in this zone, i.e., zone-1, is defined as the ratio of effective permeability at its average saturation to its viscosity, or: $\lambda_1 = (k/\mu)_1$. Zone-2 represents the geothermal reservoir fluid bank with the leading edge at a distance of r_2 from the injection well. The mobility λ of this bank in this zone, i.e., zone-2, is defined as the ratio of reservoir effective permeability as evaluated at initial water saturation to its viscosity, or: $\lambda_2 = (k/\mu)_2$.

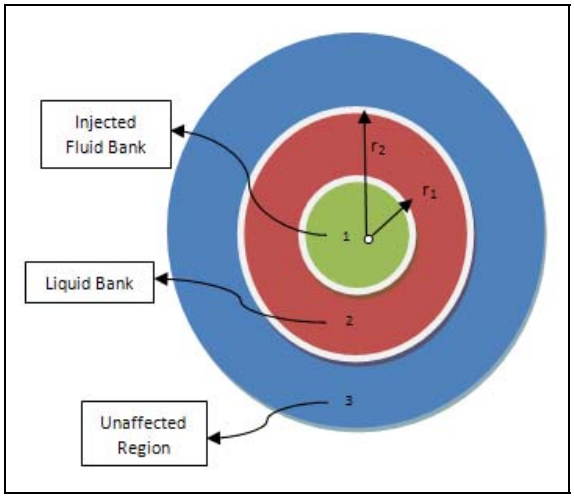

Figure 1: Schematic diagram of fluid distribution around an injection well (composite reservoir)

The assumption of a two-bank system is applicable if the reservoir is filled with liquid or if the maximum shut-in time of the falloff test is such that the radius of investigation of the test does not exceed the outer radius of the geothermal fluid bank. The ideal behaviour of the falloff test in a two-bank system as expressed in terms of the Horner plot is illustrated in figure 2.

Figure 2 shows two distinct straight lines with slopes of m_1 and m_2 that intersect at Δt_{fx}. The slope m_1 of the first line is used to estimate the effective permeability to the injected water k_w in the flooded zone and the skin factor s. It is commonly believed that the slope of the second line m_2 will yield the mobility of the geothermal fluid bank λ_2. However, Merrill et al. [3] pointed out that the slope m_2 can be used only to determine the geothermal fluid zone mobility if $r_2 > 10\ r_1$ and $(\varphi\ ct)_1 = (\varphi\ ct)_2$, and developed a technique that can be used to determine the distance r_1 and

mobility of each bank. The technique requires knowing the values of (φ ct) in the first and second zone, i.e., $(\varphi\ ct)_1$ and $(\varphi\ ct)_2$. The authors proposed equation (1):

$$\lambda = \frac{k}{\lambda} = \frac{162.6\ Q\ B}{m_2\ h} \qquad (1)$$

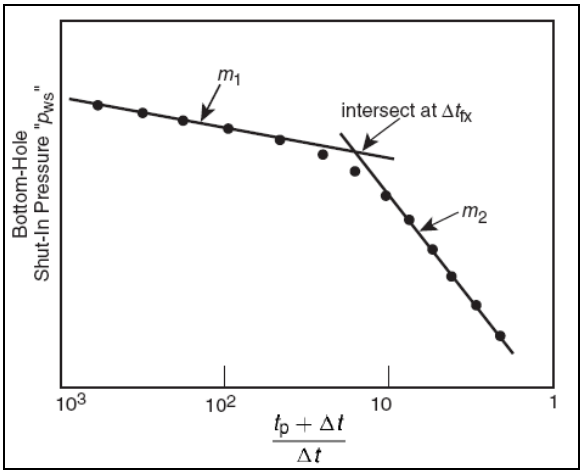

Figure 2: Pressure fall-off behaviour in a two-bank system (After Merrill, et al. 1974)

The authors also proposed two graphical correlations, as shown in Figures 3 and 4 that can be used with the Horner plot to analyse the pressure falloff data. The proposed technique is summarized by the following steps:

Step 1: Plot Δp vs. Δt on a log-log scale and determine the end of the wellbore storage effect.

Step 2: Construct the Horner plot or the MDH plot and determine m_1, m_2, and Δt_{fx}.

Step 3: Estimate the effective permeability in the first zone, i.e., injected fluid invaded zone, "zone-1," and the skin factor from equation (2) and equation (3):

$$k_1 = \frac{162.6\ q_{inj}\ B\ \mu}{|m_1|\ h} \qquad (2)$$

$$s = 1.513\left[\frac{P_{wf@\Delta t=0} - P_{1hr}}{|m_1|} - Log\left(\frac{k_1}{\emptyset \mu_1 ct_1 r_w^2}\right) + 3.2275\right] \qquad (3)$$

Step 4: Calculate the following dimensionless ratios ($\frac{m2}{m1}$ and $\frac{(\emptyset ct)1}{(\emptyset ct)2}$) with the subscripts "1" and "2" denoting zone-1 and zone-2 respectively.

Step 5: Use Figure 3 with the two dimensionless ratios of step 4 and read the mobility ratio λ_1/λ_2.

Step 6: Estimate the effective permeability in the second zone from the following equation (4):

$$k_2 = \left(\frac{\mu 2}{\mu 1}\right) * \frac{k1}{\lambda 1/\lambda 2} \qquad (4)$$

Step 7: Obtain the dimensionless time Δt_{Dfx} from Figure 4.

Step 8: Calculate the distance to the leading edge of the injected fluid bank r_1 from equation (5):

$$r_1 = \sqrt{\left[\frac{0.0002637\left(\frac{k}{\mu}\right)1}{(\emptyset ct)1} * (\Delta t_{fx} / \Delta t_{Dfx})\right]} \qquad (5)$$

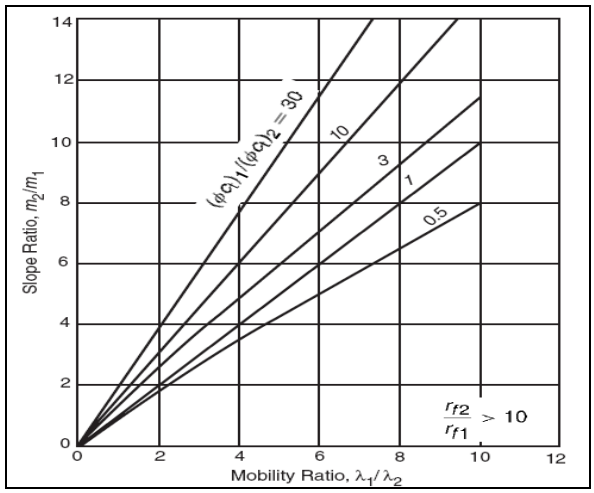

Figure 3: Relationship between mobility ratio, slope ratio and storage ratio. (After Merrill, et al. 1974)

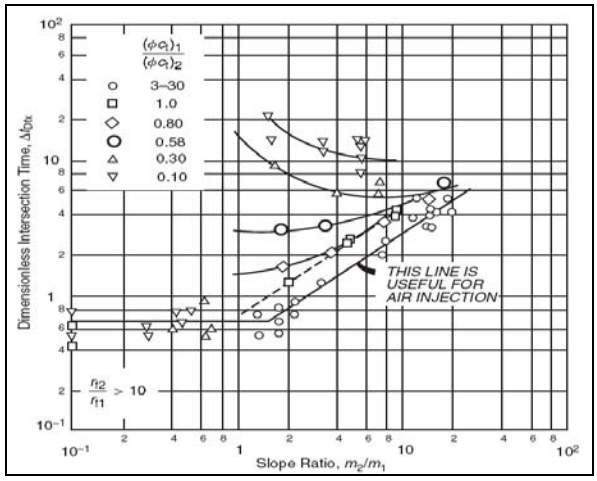

Figure 4: Correlation of dimensionless intersection time, Δt_{Dfx}, for falloff data from a two-zone reservoir. (After Merrill et al.1974).

Earlougher [1] pointed out that, as in drawdown testing, the wellbore storage has great effect on the recorded injectivity test data due to the expected large value of the wellbore storage coefficient. Earlougher recommended that all injectivity test analyses must include the log-log plot of (p_{wf} - p_i) versus injection time with the objective of determining the duration of the wellbore storage effects. The beginning of the semilog straight line, i.e., the end of the wellbore storage effects, can be estimated from Equation (6):

$$t > \frac{(200000 + 12000 * s) * C}{kh/\mu} \qquad (6)$$

Where t is the time that marks the end of wellbore storage effects (hours), μ is the viscosity (cp), k is the permeability (md), s is the skin factor and C is the wellbore storage coefficient (bbl/psi).

3. MODEL COMPARISON

In this section, one case study will be presented to obtain accurate and critical analyses for better understanding of pressure and its derivative behaviour during the water injection/fall-off tests at two different mobility ratios (M_o) of 0.3 and 4. Saphir software has been applied in this research to run the tests. The basic logic in Saphir is to guide the user through the complete interpretation process using this methodology while providing easy access to complementary side facilities. Saphir is also very much similar to a reservoir simulator in that it includes a complete multicomponent reservoir calculation.

Figure 5 shows the numerical and analytical models of the water injection/fall-off test. One can see the flow sequences including four injection periods (inj#1, 2, 4, 5) and two sequences of pressure fall-off periods (fall-off #3, 6). Note that the later injections (inj#4, 5) occur during the two pressure fall-off periods (fall-off#3, 6).

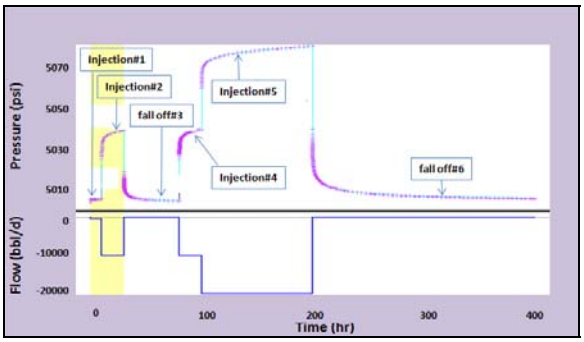

Figure 5: Variable rate flow sequences

Figure 6 shows a comparison amongst all four injection periods obtained by the Saphir numerical simulation for M_o=0.3. Note that in all these graphs the "+" and "o" signs represent the analytical data while the lines represent the simulated numerical data. According to the curves, one can see that all derivative plots (inj#1, 2 and inj#4, 5) converge to the same horizontal asymptotic trend at the late time. We do also observe three different levels for the water injection scenarios. These three different levels correspond to injected water mobility at early and late time and geothermal reservoir fluid mobility at the intermediate time. The first level may be hidden at early time for small injection quantities (Inj#1) while the last level is not seen even at small increments of time (Inj#4). The two first levels are classically interpreted corresponding to the increasing radius of investigation whereas this is not Levitan's idea [4].

Figures 7 compares the results between pressure fall-off#3 and 6 obtained by the numerical simulation. The results show that the behaviour of the pressure derivative curve during the fall-off test reflects just the fluid mobility distribution. At the early time, the derivative behaviour reflects the fluid mobility in the injected water zone near the wellbore. Thus, the longer the water bank, the longer time required for the transient pressure to become stabilised. At the later time, the behaviour of the derivative curve reflects the fluid mobility in the reservoir fluid zone ahead of Buckley-Leverett front. At the time of transition from the earlier to the later time, the behaviour of the derivative curve depends on the size of the water zone. Thus, the larger the water zone, the later the transition will occur.

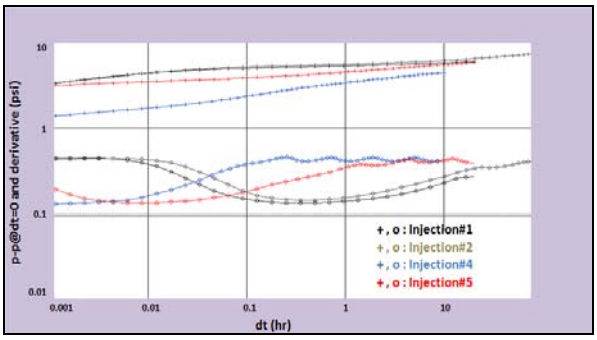

Figure 6: Comparison between p and dp for injection periods #1, 2, 4, 5 obtained by the numerical simulation for Mo =0.3.

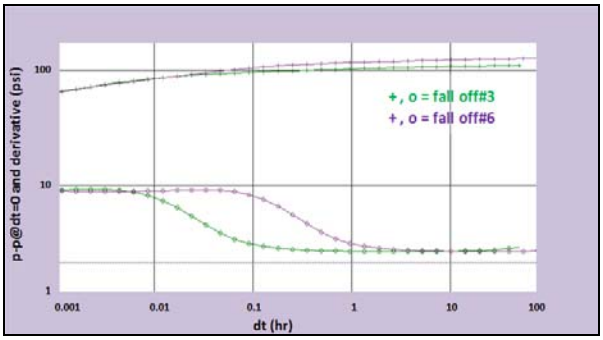

Figure 7: Comparison between p and dp for fall-off periods #3 & 6 obtained by the numerical simulation for Mo =0.3.

Similar simulations were run with the mobility ratio of 4.0 to explore the effect of viscosity on fluid movements. These results are shown in Figures 8 and 9.

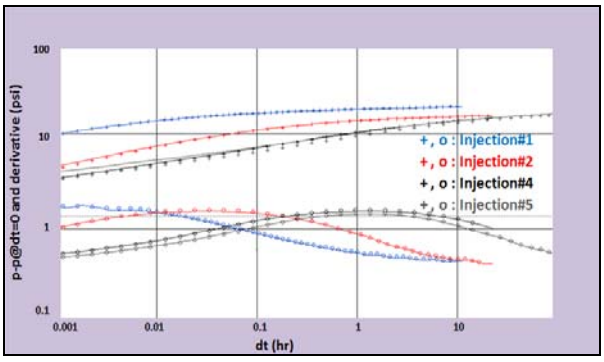

Figure 8: Comparison between p and dp for injection periods #1, 2, 4 & 5 obtained by the numerical simulation for M_o =4.0.

Based on figures 8 and 9, firstly the same behaviour was realised with inverted reservoir fluid and injected water derivative levels, secondly by increasing the mobility ratio, the numerical model appears to be more consistent with the analytical model, and thirdly by increasing the mobility ratio, the transition time from the first level to the second level has increased (there is no sharp rise).

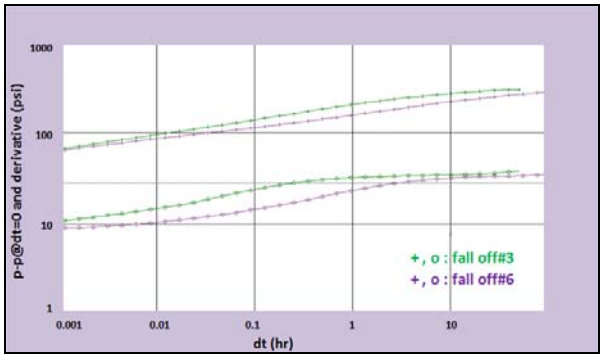

Figure 9: Comparison between pressure and pressure derivative of the two fall-off periods (fall-off #3, 6) obtained by numerical simulation for Mo =4.0.

CONCLUSIONS

This study shows that:

1. During a constant injection rate period of water into a liquid-dominated geothermal reservoir, the pressure derivative can exhibit three levels. These three different levels correspond to injected water mobility at early and late time and geothermal reservoir fluid mobility at the intermediate time.

2. During the preceding fall-off test, the pressure derivative exhibits two levels, identical to the two previous one.

3. 3. These derivative levels can be hidden either by storage effect or short time intervals.

ACKNOWLEDGMENT

I would like to thank Sinclair Knight Merz (SKM) for giving me the required time to conduct this research.

NOMENCLATURE

B = formation volume factor (B/STB)

c_t = total compressibility, psi-1

h = formation thickness, ft

k = permeability, md

M = mobility ratio

p = pressure, psi

p_i = initial reservoir pressure, psi

p_{wf} = flowing bottom hole pressure, psi

q_{inj} = injection rate, STB/D

r = radial distance, ft

r_w = wellbore radius, ft

t = time, hours

T = temperature, °C

Ø = porosity

λ = mobility, md/cp

μ = viscosity, cp

REFERENCES

J.R. Merrill, H. Kazemi and W.B. Gogarty: “Pressure Fall-off Analysis in Reservoirs with Fluid Banks”, SPE 4528

M. M. Levitan: “Application of Water Injection/Fall-off Test for Reservoir Appraisal, New Analytical Solution Method for Two Phase Variable Rate Problems”, SPE 77532, BP

M. Sabet: “Well Test Analysis”, Dallas, TX: Gulf Publishing

R. Earlougher: “Advances in Well Test Analysis”, SPE Monograph Series No. 5, 1977, 22-23, 42-45.